15.5 EFFECTS OF DEBRIS ON NEAR-SURFACE TORNADO DYNAMICS

D. C. Lewellen*, Baiyun Gong, and W. S. Lewellen
West Virginia University, Morgantown, WV.

1. INTRODUCTION

It is well recognized that strong tornadoes can transport substantial quantities of debris at high velocity and that this increases their damage potential significantly; however, there has been little study, to date, addressing whether debris loading can significantly affect the fluid-dynamic structure of the tornado itself. The debris cloud occupies only a small fraction of the tornado and the volume fraction of debris within the cloud (even at its heart) is likely very small, suggesting little impact. Our previous large-eddy simulation (LES) studies of tornado dynamics, however, have demonstrated that the properties of the near-surface inflow (where debris loading will generally be highest) critically affect the structure of the tornado corner flow (the region of highest expected winds, where the tornado core meets the surface). Given the large density ratio between, for example, dirt and air, large debris mass loadings are possible within the near surface and corner flow regions even for small volume fractions. Not only can the debris loading result in large changes in the effective total fluid density in these regions: it provides an important additional mechanism for angular momentum transport through the outward centrifuging of debris.

To address this issue we have added debris dynamics to our high-resolution, unsteady LES tornado model. This is described below, followed by preliminary results indicating that the presence of debris can significantly affect the corner flow structure.

2. DEBRIS MODEL

The basic numerical model and simulation procedures employed here are as described in Lewellen et al. (2000), except for the addition of debris. In engineering applications there are two principle methods that have been employed to introduce particulates into fully 3d unsteady flow simulations: Lagrangian tracking of individual particles or groups of particles, and treating the particles in an Eulerian framework as a second species of "fluid". We use both methods, for different purposes. A modest number of Lagrangian trajectories often suffices to determine the basic transport of particles by the flow, but when the effects of the particles on the flow become important, a much greater (often numerically prohibitive, of order a particle or more per grid cell) number is required to represent the interaction. Accordingly, we choose the "two-fluid" approach for our main goal of studying the effects of the debris on the flow structure, and use a few ($\sim$200) sample Lagrangian trajectories to provide diagnostic checks on the two-fluid debris representation. Eventually we plan on using the trajectories to represent a modest number of large debris elements (i.e., two-fluid model for dirt; Lagrangian trajectories for cars and cows).

The basic equations of the two-fluid (sometimes called "dusty gas") model are (Marble (1970)):

$$\frac{\partial(\rho u_i)}{\partial t} + \frac{\partial}{\partial x_j}(\rho u_i u_j) = \frac{\partial}{\partial x_j}(-p\delta_{ij} + \tau_{ij}) + F_{di}$$
$$\frac{\partial(\rho_d u_{di})}{\partial t} + \frac{\partial}{\partial x_j}(\rho_d u_{di} u_{dj}) = \frac{\partial \tau^d_{ij}}{\partial x_j} - F_{di} - \rho_d g \delta_{i3}$$
$$\frac{\partial u_i}{\partial x_i} = 0 \quad ; \quad \frac{\partial \rho_d}{\partial t} + \frac{\partial(\rho_d u_{di})}{\partial x_i} = 0 \quad . \qquad (1)$$

We treat the primary fluid (air) as incompressible, and the debris fluid as pressureless. The latter is a good approximation as long as the volume fraction occupied by debris is much less than one. Given the large ratio of the density of the debris itself to that of air for sand, dirt, etc. ($\sigma/\rho \gg 1$), this condition is satisfied even for debris mass loadings ($D \equiv \rho_d/\rho$) well above one. The debris falls due to gravity, and momentum is exchanged between the two fluids through the drag interaction F_d, which depends on the local velocity difference between the two fluids, and the particle Reynolds number, $Re = \rho d|\Delta u|/\mu$:

$$F_{di} = \rho_d \frac{u_{di} - u_i}{\tau_v} \qquad (2)$$
$$\tau_v \approx \frac{m}{3\pi d\mu}(1 + \frac{Re}{60} + \frac{Re/4}{1+\sqrt{Re}})^{-1}$$

The drag parameterization employed is appropriate for spherical particles of diameter d and mass m and particle Reynolds number in the range $0 < Re < 2{\cdot}10^5$. We

*Corresponding author address: D. C. Lewellen, MAE Dept. PO Box 6106, WVU, Morgantown, WV, 26506-6106; e-mail: dclewellen@mail.wvu.edu.

ignore for now any debris shape effects (e.g., lift) and rotational degrees of freedom. Within a given simulation we include only a single type of debris; eventually we may include multiple classes.

In numerically implementing (1) we treated the debris fluid in the same way as the primary fluid in our existing LES model, to the extent possible. The new 3D field variables employed are the debris mass loading D and the three components of debris momentum $\rho_d u_{di}$; the equations were discretized so that these variables are exactly conserved at the finite difference level. Limits were imposed on the debris fluxes (to avoid negative debris loadings), on the debris velocities in the debris momentum equation for very small loadings, on the time step (to satisfy Courant conditions for both the air and debris velocities), and on τ_v relative to the time step. To a large degree the drag term in the debris momentum equation plays a roll analogous to the pressure gradient term for the air, but with different (often challenging) numerical stability issues involved.

The chief physical limitation of the two-fluid model is that within each grid cell all the debris is assumed to possess the same velocity, when in reality there will be some spectrum. The approximation should work well except where debris and air velocities differ too much, and even then perform reasonably if the debris within the grid cell all have similar recent histories. The model will perform poorly in regions where two jets of debris collide, for example. The validity of the model in different regimes can be checked to some degree by comparing with results on sample Lagrangian particle trajectories.

Currently we treat the contribution of subgrid turbulence to the debris evolution (encoded in τ_{ij}^d) in the same way as for the fluid. This can be improved upon, but is adequate for our main objective of determining the leading effects of including debris within the flow, given that the resolved turbulent kinetic energy and local accelerations dominate the subgrid component at the resolution of our simulations.

To complete the debris implementation we need to specify surface boundary conditions, i.e., fluxes of debris mass and momentum to and from the surface. These will depend on the air and debris flow just above the surface, as well as on assumed surface properties. Since we are interested initially in studying large debris loadings, we concentrate on surfaces with loosely bound smaller particles (sand or dirt). The motion of particles in a surface layer with friction velocity u_* is characterized in large part by the dimensionless combination $\rho u_*^2/(\sigma dg)$. For values in the range above $\sim 10^{-2}$ and below ~ 1, the debris particles bounce along the surface in a process known as saltation (Owen, 1964), which has been much studied (and is responsible for sand dune transport, for example). It is the less well understood range above this, where the particles enter into suspension in the turbulent surface layer, that is most relevant for us. While there is much uncertainty, the debris flux in this regime appears to increase as a modest power of u_* (e.g., linearly or to the 3/2 power, see e.g., Batt et al. (1999)). Accordingly, we model that component of the debris surface flux as zero below some $O(1)$ threshold value of $\rho u_*^2/(\sigma dg)$, and proportional to ρq above it, where $q^2/2$ is the subgrid turbulent kinetic energy in our model at the first grid point above the surface. The horizontal debris momentum flux to the surface is modeled in terms of an aerodynamic roughness length in analogy to the treatment of the air momentum flux. In addition there is a negative contribution to both the debris flux and the debris momentum flux from debris falling from above and reattaching to the surface (some may bounce).

Preliminary simulations indicate that the results of this model are in at least rough quantitative agreement with wind tunnel data of the erosion of sand beds under high (30-100 m/s) winds (Batt et al., 1999). Perhaps more importantly, given the uncertainties involved, is the presence of a negative feedback that greatly reduces the sensitivity to details of the surface debris parameterization: as the debris loading in the surface layer rises, the wind velocities there fall due to the transfer of momentum to the debris through drag, and this lower velocity level then picks up less debris and reduces the loading.

3. PRELIMINARY RESULTS

Figure 1 shows velocity components from the corner flow of a simulated tornado with and without debris. In this region of the tornado the flow is highly turbulent. In order to make a quantitative comparison of the effect of debris on the flow structure we have chosen a case with outer boundary conditions (on a 2 km cube) that are steady and axisymmetric, so that we can compare axisymmetric-time averages once the tornado reaches a quasi-steady state. The case chosen is one where debris effects might be expected to be large: a strong tornado with a tight core encountering what could be roughly described as coarse sand ($d = 0.5$mm, $\sigma/\rho = 2000$) loosely bound to the surface. The results of fig. 1 show a dramatic change in structure due to the debris loading. The location of the peak mean swirl velocity of the air flow is pushed radially outward and upward and its magnitude reduced from 110 to 70 m/s. The peak mean low-level radial inflow is reduced to about 60% of its former value. The vertical air velocity structure is dramatically altered: The annular updraft is pushed outward at low levels (below $\sim$100 m), and

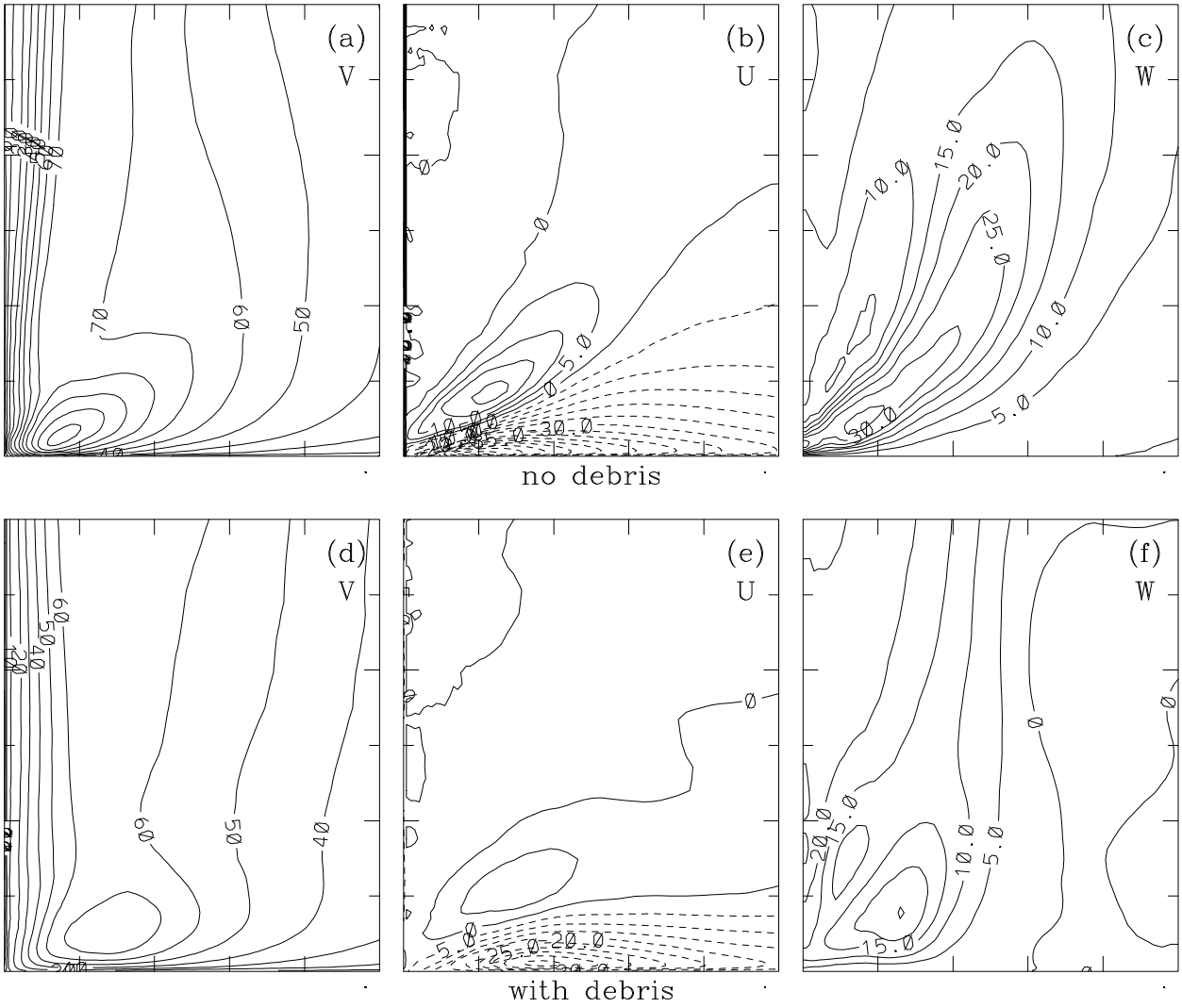

Figure 1: Axisymmetric-time averages of (a,d) swirl, (b,e) radial, and (c,f) vertical velocity components on a 250m×300m radial-vertical plane for identical simulation conditions without (a-c) and with (d-f) the presence of debris.

weakened above in favor of a stronger central updraft and a surrounding downdraft driven by falling debris.

While the addition of debris in this case generally lowers the peak wind speeds, it would be premature to conclude that it "weakens" the tornado at low levels. Figure 2a shows the mean total swirl component of momentum (air plus debris) normalized by ρ so that it may be directly compared to figures 1a and 1d. Near the surface the momentum is dominated by the debris component. The total swirl momentum reaches a mean peak value near the surface of 150m/s, well in excess of that encountered when debris is not present. The corner flow rather effectively collects debris in a low-lying annulus. The peak mean debris loading ($D \approx 4$) is buried in the saturated contours in fig. 2c. Figure 2b shows a weighted average (mean momentum normalized by mean debris density) of the debris radial velocity, which, when compared with fig. 1e, shows clearly the tendency of the debris to be centrifuged outward. For the given tornado the chosen debris is in an interesting size range: small enough to accumulate fairly high mass loadings aloft in the corner flow, but large enough that in some regions the velocity of the debris differs substantially from the air velocity.

While time averaged distributions in this case are axisymmetric, the presence of debris causes distinct spiral structures in the instantaneous distributions. Figure 3 shows an example, which also illustrates the debris driven downdraft outside of the central annular updraft.

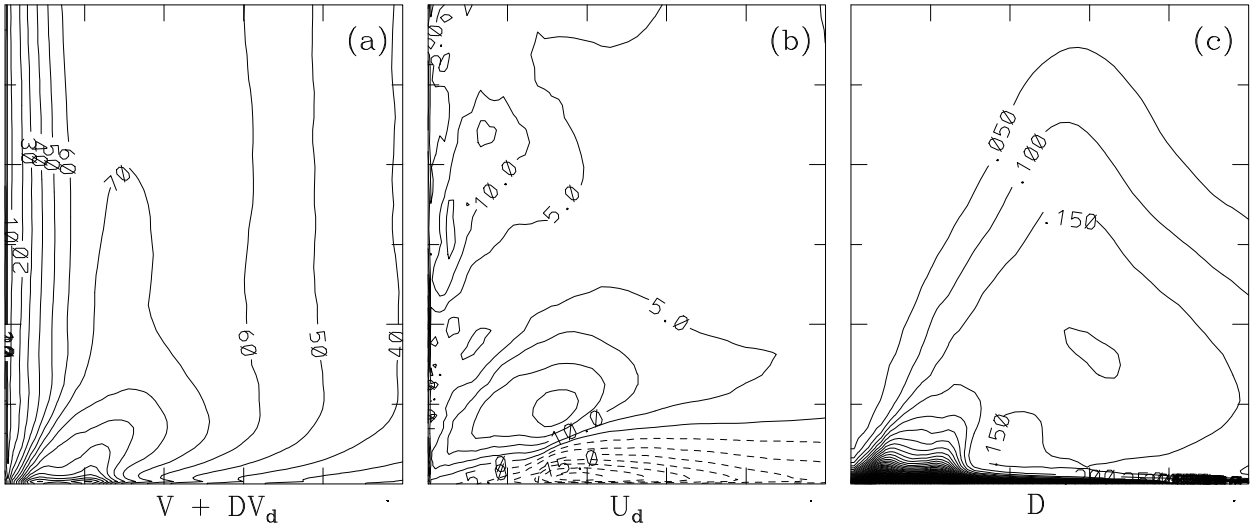

Figure 2: As in fig. 1 but showing (a) air plus debris swirl momentum normalized by air density, (b) weighted average of debris radial velocity, (c) debris loading (mass mixing ratio).

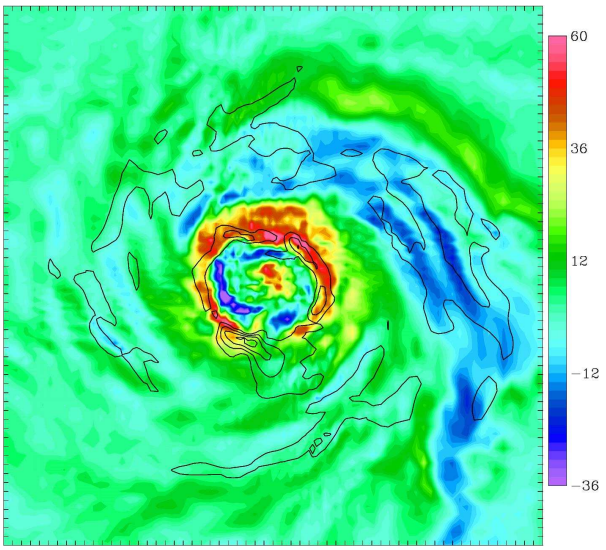

Figure 3: Instantaneous vertical wind velocity (color) and debris loading (contour lines with 0.25 interval) on a 300m × 300m horizontal slice at 50 m height through the simulated tornado of figs. 1d-f,2.

The range of tornado types, strengths, and evolutions — and the range of surface conditions/debris that they could encounter — is large, and we have only just started sampling the possibilities. We comment only briefly here on some observations to date. A simulation was performed identical to that described above except for an altered surface-debris parameterization favoring a higher debris flux. The debris cloud developed quicker, with higher mass loadings in the lowest layer; however, the negative feedback in the system is such that, once a quasi-steady state was reached, the mean statistics were nearly identical to those shown in figures 1 and 2.

The debris cloud took ∼2 min. to "mature" in the case of fig.1. This time scale can interact with the evolution time-scale of the vortex if it is rapid enough. Allowing one of the evolving "corner flow collapse" cases discussed in Lewellen and Lewellen (2002) to pick up debris, we found that the debris cloud was largest well after the tornado had passed its most intense stage, and also that the peak flow velocities at the most intense stage were reduced by a third.

The tornado of fig.1a-c has a medium corner flow swirl ratio. The corner flow swirl ratio can be interpreted (Lewellen et al., 2000) as the ratio of a swirl velocity to a flow through velocity within the surface-corner-core flow. The debris centrifuging in the surface layer impedes the radial inflow of air to a greater extent than it impedes the swirling component. It would be natural then for the introduction of debris to effectively increase the corner flow swirl ratio; the results in fig.1 seem to bear this out. While we have not gathered long time statistics for cases with other swirl ratios, initial simulations of high and low corner flow swirl ratio tornadoes support this conclusion as well. In particular, when a simulated low-swirl tornado (characterized by a central vertical jet off the surface capped by a vortex breakdown) accumulates debris, the central jet is replaced by an annular updraft as in a "medium swirl" vortex.

Preliminary indications are that the addition of a sizable translation velocity to the tornado does not in-

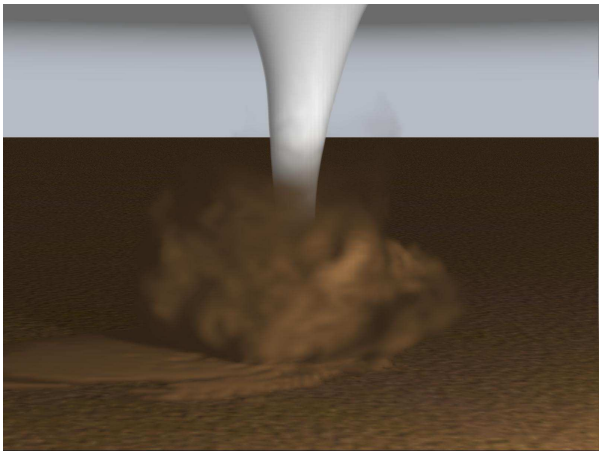

Figure 4: Visual appearance of the debris and funnel clouds from a simulated medium swirl F3-F4 tornado translating from left to right at 15 m/s, ingesting 1mm diameter "sand" from the surface.

hibit its capacity to collect and transport small-scale debris, although it makes the surface collection significantly non-axisymmetric. At least qualitatively, the visual appearance of the simulated debris cloud, e.g., fig. 4, looks realistic, particularly when animated. Note that the light colored patch below and to the left of the main debris cloud in fig. 4 represents debris in the near-surface inflow layer.

4. DISCUSSION

Much work remains to be done to more carefully test and improve our modeling of debris within tornadoes, and to assess its effects. Our preliminary results are enough, however, to indicate the potential importance of this effort: at least in some regimes it appears that the accumulation of small-scale debris within the surface layer and corner flow can significantly alter the flow structure of the tornado vortex within a few hundred meters of the surface.

This initial work suggests many questions to explore: Are there conditions (e.g., very low swirl ratio) in which adding debris raises the flow velocities? Which types of debris accumulate most effectively in the corner flow? What happens when a full spectrum of debris sizes is present? What are the effects of surface variations? Are there critical unsteady effects? Do debris effects preclude the presence of a low swirl surface jet in a strong tornado?

While our primary goal in this work is to study the effect of debris on the tornado structure itself, there are important secondary objectives as well. The debris loading and momentum near the surface will have a significant impact on the destructive capability of the tornado. The signal from high resolution Doppler radars is also strongly affected by the debris loading, distribution, and velocity relative to the air-flow velocity (c.f., figs. 1e and 2b). Finally, the debris cloud and condensation funnel are the primary observational signatures of tornadoes; realistically simulating their appearance may allow us to correlate the visual structure of some tornadoes, as extensively recorded on video, with the precisely determined structure and velocity measurements of our simulations.

5. ACKNOWLEDGMENTS

This research was supported by National Science Foundation Grant ATM236667. We thank Paul Lewellen for rendering the graphic in fig. 4 from our simulation data.

References

Batt, R. G., M. P. Petach, S. A. Peabody, and R. R. Batt, 1999: Boundary layer entrainment of sand-sized particles at high speed. *J. Fluid Mech.*, **392**, 335–360.

Lewellen, D. C., and W. S. Lewellen, 2002: Near-surface intensification during unsteady tornado evolution. *Preprints, 21th Conference on Severe Local Storms*, Amer. Meteor. Soc., San Antonio, TX, 481-484.

Lewellen, D. C., W. S. Lewellen, and J. Xia, 2000: The influence of a local swirl ratio on tornado intensification near the surface. *J. Atmos. Sci.*, **57**, 527–544.

Marble, F. E., 1970: Dynamics of dusty gases. *Ann. Rev. Fluid Mech.*, **2**, 397–446.

Owen, P. R., 1964: Saltation of uniform grains in air. *J. Fluid Mech.*, **20**, 225–242.